Received: 25 March 2019 | Revised: 22 August 2019 | Accepted: 22 August 2019

DOI: 10.1111/jace.16772

Journal of the American Ceramic Society

RAPID COMMUNICATION

Fabrication of porous thick films using room-temperature aerosol deposition

Neamul H. Khansur[1] | Udo Eckstein[1] | Matej Sadl[2,3] | Hana Ursic[2,3] | Kyle G. Webber[1]

[1]Department of Materials Science and Engineering, Friedrich-Alexander-Universität Erlangen-Nürnberg, Erlangen, Germany

[2]Electronic Ceramics Department, Jožef Stefan Institute, Ljubljana, Slovenia

[3]Jožef Stefan International Postgraduate School, Ljubljana, Slovenia

Correspondence
Neamul H Khansur, Department of Materials Science and Engineering, Friedrich-Alexander-Universität Erlangen-Nürnberg, 91058 Erlangen, Germany.
Email: neamul.khansur@fau.de

Funding information
Deutsche Forschungsgemeinschaft, Grant/Award Number: WE4972/4-DE1598/5 and WE4972/2; DAAD, Grant/Award Number: 57402168; Slovenian Research Agency, Grant/Award Number: BI-DE-18/19-012, PR-08977 and P2-0105

Abstract

A novel technique for the rapid room-temperature deposition of porous ceramic, glass, or metal thick films using the aerosol deposition (AD) method is presented. The process is based on the co-deposition of the desired film material and a second water-soluble constituent, resulting in a ceramic-ceramic composite. Following the subsequent removal of water-soluble end member, a network of pores is retained. To demonstrate the process, porous $BaTiO_3$ thick films were fabricated through co-deposition with NaCl. Microstructural images show the clear development of a porous structure, which was found to enhance the dielectric properties over dense thick films, possibly related to the lower extent of internal residual stress. This simple but highly effective porous structure fabrication can be applied to any film and substrate material stable in water and is promising for the application of AD-processed films in gas sensors, solid oxide fuel cells, and humidity sensors.

KEYWORDS

ceramic matrix composites, dielectric materials/properties, porous materials, sensors

1 | INTRODUCTION

The aerosol deposition (AD) method[1] has gained significant interest as it facilitates the rapid fabrication of ceramic films on different ceramic, metallic, glass, and polymeric substrates at room temperature. The AD is a type of low-temperature spray deposition technique, where submicron particles are aerosolized and carried through a specifically designed nozzle using a carrier gas to impact on the substrate. It is argued that the deposition process involves particle fracture and impact consolidation without any significant rise of local temperature.[1] Due to the impact consolidation mechanisms, AD-processed films exhibit nanograined microstructure with relatively high density.[2] In addition, AD-processed films possess high internal residual stress, on the order of ~GPa, related to the deposition process.[3–7]

Dense ceramic films with enhanced functional properties as well as mechanical stability are useful for numerous applications, such as energy harvesters, sensors, microelectronics.[8,9] However, for some specific applications the optimized properties are realized by the presence of controlled porosity in the microstructure. In fact, fabrication and understanding of electromechanical behavior in porous bulk ceramic are a significant area of academic and industrial interest.[10–14] Additionally, ceramic films with porous microstructure are also essential for numerous practical applications. For instance, the gas-sensing properties and humidity sensing efficiency are profoundly affected by the density of the functional ceramic films.[15,16] In addition, solid-oxide fuel cells also requires a porous electrode layer for both the cathode and anode to facilitate efficient operation.[17] For these reasons, a number of previous investigations have focused on developing porous

films using the AD method.[18,19] Ryu et al[19] used a β-tricalcium phosphate/TiO_2 composite and an acid leaching step to create a porous structure, demonstrating enhanced photocatalytic activity of the porous TiO_2 film. It has also been found that adding a small amount of polymer to the ceramic matrix and subsequent high-temperature heating of the as-deposited film can reduce the internal residual stress and induce porosity in the structure.[20] Recently, a Japanese patent was filed that mentioned the fabrication of porous AD films for dye-sensitized solar cell using nanoparticles of water-soluble materials.[21] In this work, however, we demonstrate a simple way to prepare AD-processed porous structure without requiring any heat-treatment or acidic chemicals. Importantly, this technique can be applied to any water-stable substrate and film material, such as ceramics, metals, and glasses, which opens the possibilities for application in numerous technologies and engineered structures. To demonstrate the facile green fabrication route, we used water-soluble NaCl powder and $BaTiO_3$ to prepare a ceramic-ceramic composite. The microstructure and relative dielectric permittivity of an AD-processed dense $BaTiO_3$ film of ~16 μm thickness was compared with that of an AD-processed porous $BaTiO_3$ film.

2 | EXPERIMENTAL PROCEDURE

Commercially available $BaTiO_3$ (Helsa-automotive GmbH & Co. KG) and NaCl powder were used in this work. NaCl powder was milled using cyclohexane to optimize the median particle size, d_{50} ≈1.2 μm for the deposition. As-received $BaTiO_3$ powder was milled using a rolling mill to obtain the median particle size d_{50} ≈ 1 μm. The NaCl and $BaTiO_3$ powders were dry mixed with a ratio of 70 vol% NaCl and 30 vol% $BaTiO_3$. The NaCl/$BaTiO_3$ composite powder was codeposited on a stainless steel substrate (SUS 304) using the AD process.[7] Details of the AD process parameters can be found in Table 1. Following deposition, the NaCl/$BaTiO_3$ composite film was washed using distilled water in an ultrasonic bath for 5 minutes. The washed sample was air dried for approximately 12 hours at 100°C before measurements. The cross-section of the sample was prepared using sequential grinding, polishing, and additional fine polishing with colloidal silica suspension for 90 minutes. Microstructures were observed using a field-emission scanning electron microscope (FE-SEM, JSM-7600F). The microstructure was analyzed to obtain an estimation of the fraction of porous area in the film using ImageJ.[22] The temperature-dependent dielectric permittivity over the range from room temperature to 300°C was measured using an automated system whereby an impedance analyzer Keysight Model E4980AL and a furnace (LE 4/11 3216, Nabertherm GmbH) were controlled by a LabView program. During testing, the SUS304 substrate acted as the bottom electrode, while a top Pt (area of 5 × 4 mm) electrode was sputtered on the opposite side of the film. The sample was electrically contacted with the 4-point measurement technique using Pt wires, which were electrically shielded by Inconel tubing to minimize external parasitic signals.

TABLE 1 AD film deposition parameters

Average starting particle size	1 and 1.2 μm
Substrate thickness	1 mm
Substrate material	Stainless steel (SUS 304)
Carrier gas	N_2
Size of the nozzle orifice	10 × 0.5 mm
Pressure in the deposition chamber	~3 mbar
Carrier gas flow rate	4.0 l/min
Deposition area	10 × 8 mm
Film thickness	~16 μm

3 | RESULTS AND DISCUSSION

The cross-sectional images of the as-processed dense $BaTiO_3$ and porous $BaTiO_3$ films, that is, after the removal of NaCl, are shown in Figure 1A,B, respectively. A significant difference in the microstructure is visible, most notably an increase in the number and size of the visible pores through the thickness of the film. The observed pores also appear elongated parallel to the substrate surface. This elongation is possibly related to the impact consolidation mechanisms of AD. As porosity can be observed through the full thickness of the $BaTiO_3$ film, it is expected that the porous network fully penetrates the film. However, it is important to note that how much NaCl is fully embedded in the BT matrix and cannot be removed with the washing process remains unclear. It is likely that the resulting porous film is a combination of 0-3 and 3-3 connectivity, where additional studies are required to accurately determine the ratio of each. It should be mentioned here that the deposition parameters and particle morphology of the $BaTiO_3$ powder was the same for both cases. Additional SEM image (Figure S1) reveals that a size reduction of the starting ceramic particles took place during the co-deposition of $BaTiO_3$/NaCl powder. Moreover, the AD process-induced crystallite size reduction was also confirmed for both the dense and porous film (Figure S4). These observations further confirmed the impact consolidation process in the $BaTiO_3$/NaCl codeposited porous film. Additionally, our previous study showed that NaCl itself can be deposited using AD process where impact consolidation phenomenon occurred.[23]

In order to determine the pore content, the cross-sectional microstructure of the dense and porous BT film was analyzed

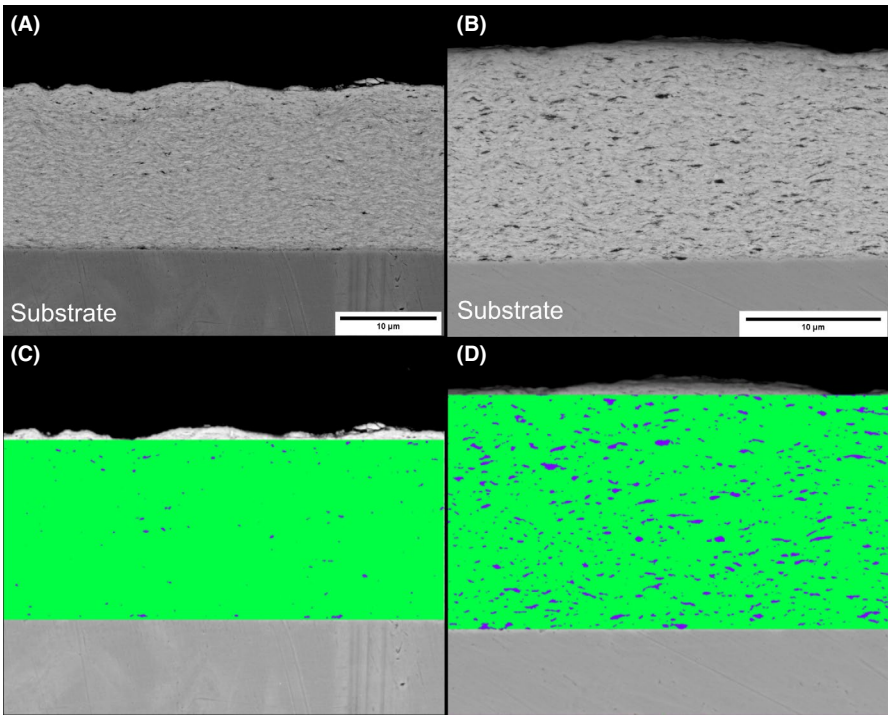

FIGURE 1 Cross-sectional micrographs of a dense (A) and a porous (B) $BaTiO_3$ film deposited with AD. Analyzed area fraction of a dense (C) and a porous film (D). A calculated porous area fraction of 1.7% and 11.8% were obtained, respectively [Color figure can be viewed at wileyonlinelibrary.com]

(Figure 1C,D). From this analysis of the microstructure, a porosity of 1.7% ± 1% and 11.8% ± 2.7% was estimated for dense and porous AD films, respectively. It should be mentioned here that the ceramic specimen with a density of ≤90% of theoretical density can be considered to exhibit open porosity, that is, interconnected pores.[24,25] In our case, the estimated porosity of approximately 12% further indicates the occurrence of open porosity. An average pore size (feret diameter) of 0.10 ± 0.05 μm (176 pores) and 0.14 ± 0.07 μm (498 pores) for dense and porous BT films were estimated. It should be highlighted that although average pore size of the porous BT is not significantly different from the dense BT film, the number of pores is almost four times greater and also they are more homogeneously distributed. It is important to note that although the average pore size is ~0.1 μm the pore size is not homogenous, that is, a number of pores larger than the average size is clearly visible. For a better analysis of porous structure, it will be ideal to investigate using micro-CT or spectroscopic ellipsometry. Nevertheless, our analysis gives a semi-quantitative estimation of the extent of porosity in the film. It should be noted here that, despite the use of 70 vol% NaCl, the estimated porosity using a microstructure image is only approximately 12%. This is possibly related to the difference in deposition efficiency of NaCl and $BaTiO_3$. It is reasonable that for a given carrier gas flow rate NaCl and BT will have different impact velocities due to the difference in density of NaCl (2.16 g/cm^3) and $BaTiO_3$ (6.02 g/cm^3). It is considered that for the deposition of AD film, a window for particle impact velocity of 150-500 m/s is required.[2] Therefore, variation in impact velocities can affect the particle deposition efficiency. Another possibility is that the dry mixing of the constituent particles was not sufficient to homogenously distribute the NaCl and $BaTiO_3$. Wet mixing of NaCl and BT using cyclohexane could be beneficial to improve the homogeneity.

AD-deposited BT ceramic films are of significant interest for humidity sensing applications.[15,16] The efficiency of the humidity sensor prepared by AD-processed film can be significantly improved by the porous microstructure. The porous structure obtained using a simple method in our work can be helpful to explore further humidity sensing properties of other material systems. The temperature-dependent dielectric permittivity of as-processed and heat-treated BT films, both dense and porous, is shown in Figure 2. The porous BT film displayed a room-temperature dielectric permittivity value nearly twice that of the dense film. This enhanced permittivity is possibly related to the lower internal stress in the porous film. Previous reports on AD-processed film have shown that the porous films as well as ceramic/polymer composite films exhibit lower internal stresses than the regular processed AD film.[26–28] In addition, although we have not observed any significant difference in the grain size as well as in the crystallite size of dense and porous $BaTiO_3$ film (Figures S1-S4), it is known that the AD-processed film exhibits inhomogeneous grain size. Therefore, it is possible that the presence of NaCl, that is, co-deposition of $BaTiO_3$/NaCl shifted the $BaTiO_3$ grain size distribution toward larger grains and resulted in an increase in permittivity. It should be mentioned here that the AD-processed dielectric ceramic films intrinsically show lower dielectric permittivity than their bulk counterpart and is possibly related to the fine-grained microstructure.[29,30] In addition, previous studies on the stress-dependent dielectric

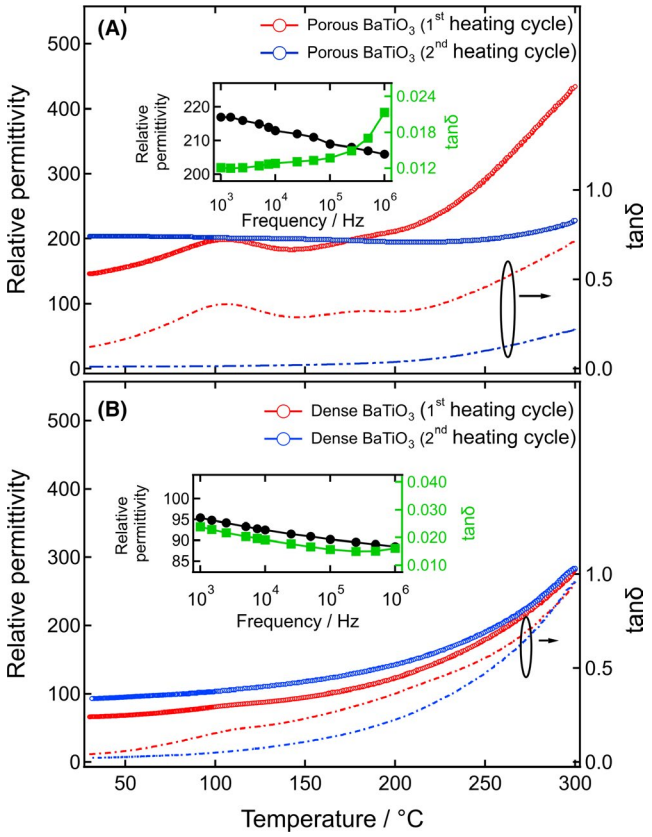

FIGURE 2 Temperature-dependent dielectric permittivity of the as-processed (1st heating cycle) and dried (2nd heating cycle) (A) porous $BaTiO_3$ and (B) dense $BaTiO_3$ measured at 1 kHz. Frequency-dependent room-temperature (~20°C) dielectric permittivity of the porous and dense film after heat treatment up to 300°C is shown as the inset in (A) and (B), respectively [Color figure can be viewed at wileyonlinelibrary.com]

permittivity of $BaTiO_3$ have shown an increase in the Curie temperature and a more diffuse phase transition.[31] The observed dielectric anomaly at approximately 100°C in the as-processed porous BT film is likely related to water incorporation, which could have occurred during the washing process to remove NaCl. No such anomaly was observed for the second heating cycle, indicating that the water was removed. A similar minor dielectric peak at 100°C was also observed in the dense as-processed film, likely also related to water incorporation through, for example, humidity. Interestingly, the permittivity value for the porous BT film is higher than the regular dense BT film of similar thickness even after heat treatment, indicating that the higher permittivity exhibited in the porous BT film is not solely related to the water content. The frequency-dependent dielectric permittivity of the thermally annealed porous $BaTiO_3$ film is shown in inset of Figure 2A. It can be seen that within the broad frequency range the room-temperature permittivity value does not change significantly.

4 | CONCLUSIONS

We developed a simple fabrication method for porous ceramic thick films, which can also be applied to other non–water-soluble film and substrate materials. This cost-effective and rapid method involves the co-deposition of a water-soluble and a non-water soluble end member, resulting in a ceramic-ceramic composite. After removal of the water-soluble end member, a network of pores is retained, which can have significant influence on various industrial applications. The results of $BaTiO_3$ films deposited on steel were presented, where a porosity of approximately 12% were found to increase the relative permittivity.

ACKNOWLEDGMENTS

NHK, UE, and KGW gratefully acknowledge financial support for this work from the Deutsche Forschungsgemeinschaft under WE4972/4-DE1598/5 and WE4972/2, as well as the support of the DAAD under project 57402168 as part of the PPP Slovenian Programme. HU and MS acknowledge support from the Slovenian Research Agency (bilateral project BI-DE-18/19-012, PR-08977, P2-0105) and Ultracool Director's fund 2017. HU and MS also thank J. Cilensek for assistance in the laboratory. NHK and UE also thank Jonas Biggemann for the helpful discussions on the analysis of porous microstructures.

ORCID

Neamul H. Khansur https://orcid.org/0000-0001-8769-3329
Udo Eckstein https://orcid.org/0000-0001-9546-8463
Matej Sadl https://orcid.org/0000-0003-1497-5610

REFERENCES

1. Akedo J. Aerosol deposition of ceramic thick films at room temperature: densification mechanism of ceramic layers. J Am Ceram Soc. 2006;89(6):1834.
2. Akedo J. Room temperature impact consolidation (RTIC) of fine ceramic powder by aerosol deposition method and applications to microdevices. J Therm Spray Technol. 2008;17(2):181.
3. Iwata A, Akedo J, Lebedev M. Cubic aluminum nitride transformed under reduced pressure using aerosol deposition method. J Am Ceram Soc. 2005;88(4):1067–9.
4. Adamczyk J, Fuierer P. Compressive stress in nano-crystalline titanium dioxide films by aerosol deposition. Surf Coat Technol. 2018;350:542–9.
5. Schubert M, Exner J, Moos R. Influence of carrier gas composition on the stress of Al_2O_3 coatings prepared by the aerosol deposition method. Materials. 2014;7(8):5633.

6. Khansur NH, Eckstein U, Riess K, Martin A, Drnec J, Deisinger U, et al. Synchrotron x-ray microdiffraction study of residual stresses in $BaTiO_3$ films deposited at room temperature by aerosol deposition. Scripta Mater. 2018;157:86–9.
7. Khansur NH, Eckstein U, Benker L, Deisinger U, Merle B, Webber KG. Room temperature deposition of functional ceramic films on low-cost metal substrate. Ceram Int. 2018;44(14):16295–301.
8. Hanft D, Exner J, Schubert M, Stöcker T, Fuierer P, Moos R. An Overview of the aerosol deposition method: process fundamentals and new trends in materials applications. J Ceram Sci Tech. 2015;06(03):147.
9. Muralt P. Ferroelectric thin films for micro-sensors and actuators: a review. J Micromech Microeng. 2000;10(2):136.
10. Olariu CS, Padurariu L, Stanculescu R, Baldisserri C, Galassi C, Mitoseriu L. Investigation of low field dielectric properties of anisotropic porous Pb(Zr, Ti)O_3 ceramics: experiment and modeling. J Appl Phys. 2013;114(21):214101.
11. Roscow JI, Lewis R, Taylor J, Bowen CR. Modelling and fabrication of porous sandwich layer barium titanate with improved piezoelectric energy harvesting figures of merit. Acta Mater. 2017;128:207–17.
12. Zhang Y, Roscow J, Xie M, Bowen C. High piezoelectric sensitivity and hydrostatic figures of merit in unidirectional porous ferroelectric ceramics fabricated by freeze casting. J Eur Ceram Soc. 2018;38(12):4203–11.
13. Yap EW, Glaum J, Oddershede J, Daniels JE. Effect of porosity on the ferroelectric and piezoelectric properties of $(Ba_{0.85}Ca_{0.15})(Zr_{0.1}Ti_{0.9})O_3$ piezoelectric ceramics. Scripta Mater. 2018;145:122–5.
14. Zhang Y, Roscow J, Lewis R, Khanbareh H, Topolov VY, Xie MY, et al. Understanding the effect of porosity on the polarisation-field response of ferroelectric materials. Acta Mater. 2018;154:100–12.
15. Liang J-G, Wang C, Yao Z, Liu M-Q, Kim H-K, Oh J-M, et al. Preparation of ultrasensitive humidity-sensing films by aerosol deposition. ACS Appl Mater Interfaces. 2018;10(1):851–63.
16. Liang J-G, Kim E-S, Wang C, Cho M-Y, Oh J-M, Kim N-Y. Thickness effects of aerosol deposited hygroscopic films on ultra-sensitive humidity sensors. Sens Actuators B Chem. 2018;265:632–43.
17. Echigo M, Ohnishi H, Manabe K, Yamazaki O, Minami K, Tsuda Y inventors; US Patents, assignee. Electrochemical Element, Solid Oxide Fuel Cell, and Methods for Producing the Same 2017.
18. Hirose S, Ezuka Y, Akedo J, Kunugi S, Yoguchi S, Nakajima S inventors; National Institute of Advanced Industrial Science and Technology, Tokyo (JP); Sekisui Chemical Co. Ltd., Osaka (JP), Assignee. Method for forming a dye-sensitized solar cell having a porous film of an inorganic substance on a base material by spraying dry fine particles of an inorganic substance on the base material, Patent No. US 9721733 B1.2017.
19. Ryu J, Hahn B-D, Choi J-J, Yoon W-H, Lee B-K, Choi JH, et al. Porous photocatalytic TiO_2 thin films by aerosol deposition. J Am Ceram Soc. 2009;93(1):55–8.
20. Kim H-J, Kim Y-H, Lee J-W, Nam S-M, Yoon YJ, Kim J-H. Residual stress relief in Al_2O_3–poly-tetra-fluoro-ethylene hybrid thick films for integrated substrates using aerosol deposition. J Nanoelectron Optoelectron. 2012;7(3):287–91.
21. Anzai J. inventor. Sekisui Chemical Co., Ltd., AssigneeMethod for producing porous membrane (in Japanese). Japan patent JP6134106B2. 2017.
22. Schindelin J, Arganda-Carreras I, Frise E, Kaynig V, Longair M, Pietzsch T, et al. Fiji: an open-source platform for biological-image analysis. Nat Methods. 2012;9(7):676–2.
23. Khansur NH, Eckstein U, Li Y, Hall DA, Kaschta J, Webber KG. Revealing the effects of aerosol deposition on the substrate-film interface using NaCl coating. J Am Ceram Soc. 2019;102(10):5763–1.
24. Kikuchi T, Takahashi T, Nasu S. Porosity dependence of thermal conductivity of uranium mononitride. J Nucl Mater. 1973;45(4):284–92.
25. Schulz B. Thermal conductivity of porous and highly porous materials. High Temp - High Pressures. 1981;13(6):649–60.
26. Kim Y-H, Kim H-J, Koh J-H, Ha J-G, Yun Y-H, Nam S-M. Fabrication of $BaTiO_3$-PTFE composite film for embedded capacitor employing aerosol deposition. Ceram Int. 2011;37(6):1859–64.
27. Kim HJ, Yoon YJ, Kim JH, Nam SM. Application of Al_2O_3-based polyimide composite thick films to integrated substrates using aerosol deposition method. Mater Sci Eng B. 2009;161(1):104–8.
28. Akedo J, Park J-H, Kawakami Y. Piezoelectric thick film fabricated with aerosol deposition and its application to piezoelectric devices. Jpn J Appl Phys2018;57(7S1):07LA02.
29. Kim H-K, Lee S-H, Kim SI, Lee CW, Yoon JR, Lee S-G, et al. Dielectric strength of voidless $BaTiO_3$ films with nano-scale grains fabricated by aerosol deposition. J Appl Phys. 2014;115(1):014101.
30. Hoshina T, Furuta T, Kigoshi Y, Hatta S, Horiuchi N, Takeda H, et al. Size effect of nanograined $BaTiO_3$ ceramics fabricated by aerosol deposition method. Jpn J Appl Phys. 2010;49(9S):09MC2.
31. Schader FH, Aulbach E, Webber KG, George A, Rossetti J. Influence of uniaxial stress on the ferroelectric-to-paraelectric phase change in barium titanate. J Appl Phys. 2013;113(17):174103.

SUPPORTING INFORMATION

Additional supporting information may be found online in the Supporting Information section at the end of the article.

How to cite this article: Khansur NH, Eckstein U, Sadl M, Ursic H, Webber KG. Fabrication of porous thick films using room-temperature aerosol deposition. *J Am Ceram Soc*. 2020;103:43–47. https://doi.org/10.1111/jace.16772